Nuclear Materials and Energy 12 (2017) 575–581

Contents lists available at ScienceDirect

Nuclear Materials and Energy

journal homepage: www.elsevier.com/locate/nme

Surface modification of He pre-exposed tungsten samples by He plasma impact in the divertor manipulator of ASDEX Upgrade

S. Brezinsek[a,*], A. Hakola[b], H. Greuner[c], M. Balden[c], A. Kallenbach[c], M. Oberkofler[c], G. De Temmerman[d], D. Douai[e], A. Lahtinen[b], B. Böswirth[c], D. Brida[c], R. Caniello[f], D. Carralero[c], S. Elgeti[c], K. Krieger[c], H. Mayer[g], G. Meisl[c], S. Potzel[c], V. Rohde[c], B. Sieglin[c], A. Terra[a], R. Neu[c], Ch. Linsmeier[a], the EUROfusion MST1 Team [1,2]

[a] Forschungszentrum Jülich GmbH, Institut für Energie- und Klimaforschung - Plasmaphysik, Partner of the Trilateral Euregio Cluster, 52425 Jülich, Germany
[b] VTT Technical Research Centre of Finland Ltd., P.O. Box 1000, 02044 VTT, Finland
[c] Max-Planck-Institut für Plasmaphysik, D-85748 Garching, Germany
[d] ITER Organization, Route de Vinon-sur-Verdon - CS 90 046 - 13067 St Paul Lez Durance Cedex, France
[e] CEA, IRFM, F-13108 Saint-Paul-lez-Durance, France
[f] Istituto di Fisica del Plasma - CNR, Via R. Cozzi 53, 20125 Milan, Italy
[g] Culham Centre for Fusion Energy, Culham Science Centre, Abingdon, OX14 3DB, UK

ARTICLE INFO

Article history:
Received 24 July 2016
Revised 27 September 2016
Accepted 1 November 2016
Available online 23 December 2016

Keywords:
PSI
ASDEX Upgrade
ITER
W divertor
W nanostructure
Helium

ABSTRACT

Tungsten (W) will be used as material for plasma-facing components (PFCs) in the divertor of ITER and interact with Helium (He) ions either from initial He plasma operation or from Deuterium-Tritium (DT) fusion reactions in the active operation phase. Laboratory experiments reported that in a specific operational window of impact energy, ion fluence, and surface temperature ($E_{in} \geq 20$ eV, $\phi \geq 1 \times 10^{24}$ $He^{+}m^{-2}$, $T_{surf} \geq 1000$ K) a modification of W surfaces occurs resulting in the formation of He-induced W nanostructures. Experiments in ASDEX Upgrade H-mode plasmas ($B_t = 2.5$ T, $I_p = 0.8$ MA, $P_{aux} \simeq 8.0$ MW) in He have been carried out to investigate in detail (a) the potential growth of W nanostructures on pre-damaged W samples incorporating He nanobubbles, and (b) the potential ELM-induced erosion of W nanostructure. Both W surface modifications were generated artificially in the GLADIS facility by He bombardment of W samples at $E_{in} = 37$ keV (a) to $\phi \simeq 0.75 \times 10^{24}$ $He^{0}m^{-2}$ at $T_{surf} \simeq 1800$ K and (b) $\phi \simeq 1 \times 10^{24}$ $He^{0}m^{-2}$ at $T_{surf} \simeq 2300$ K prior to exposure in the divertor manipulator of ASDEX Upgrade. Though in part (a) conditions of W nanostructure growth with a total He ion fluence of $\phi \simeq 1.6 \times 10^{24}$ $He^{+}m^{-2}$ and peak He ion impact energies above 150 eV were met, no growth could be detected. In part (b) lower density plasmas with more pronounced type I ELMs, carrying energetic He ions in the *keV* range, were executed with the strike-line positioned on 2 µm thick W nanostructure accumulating a fluence of $\phi \simeq 0.8 \times 10^{24}$ $He^{+}m^{-2}$. Post-mortem analysis revealed that co-deposition by predominantly W, and Boron (B), eroded at the main chamber wall and transported into the divertor, took place on all W samples. Erosion of W nanostructure or its formation was hindered by the fact that the outer divertor at the location of the samples was turned under these He plasma conditions into a net deposition zone by W, B and Carbon (C) ions. The surface morphology with large roughness and effective surface area act as a catcher for the impinging impurities. Thus, apart from operation in the existence diagram of W nanostructure with respect to T_{surf}, ϕ, and E_{in}, also the impinging impurity flux contribution needs to be considered in predictions concerning the formation of W nanostructures.

* Corresponding author.
E-mail address: s.brezinsek@fz-juelich.de (S. Brezinsek).

[1] see http://www.euro-fusionscipub.org/mst1.

[2] This work has been carried out within the framework of the EUROfusion Consortium and has received funding from the Euratom research and training programme 2014–2018 under grant agreement No 633053. The views and opinions expressed herein do not necessarily reflect those of the European Commission.

http://dx.doi.org/10.1016/j.nme.2016.11.002

1. Introduction

Tungsten (W) will be used as material for plasma-facing components (PFCs) in the ITER divertor [1] due to its good power handling properties, high melting point as well as low fuel retention and sputtering in plasmas with hydrogenic fuel [2]. These advantages have been successfully demonstrated in deuterium (D) plasmas in ASDEX Upgrade and JET with full W divertors [3]. However, operation in helium (He) or mixed D/He plasmas have barely been executed in devices with W PFCs and are of vital importance as e.g. ITER plans to operate in He plasmas during the non-active start-up phase and will produce fusion α-particles by DT reactions in the active phase.

Laboratory experiments, i.e. in linear plasma devices and neutral beam facilities, reported on microstructure modifications under energetic He ion or atom bombardment of W PFCs resulting in W nanostructures (W fuzz or W dendrils or W coral-like structure) [4,5]. The required W surface and He ion (He plasma) conditions for the formation of W nanostructure have been summarised in [6] including the identification of He nanobubbles in W as potential precursor. W nanostructures are formed when the impact He ion energy E_{in} exceeds 20 eV, the surface temperature T_{surf} exceeds 1000 K, and the fluence ϕ is larger than approximately 1×10^{24} $He^{+}m^{-2}$. Recent studies [8] identified a threshold for their formation at low fluence. These W nanostructures could potentially compromise power handling, impact the fuel retention [7], and induce finally dust formation from W plasma-facing components [2]. A critical question is if such surface modifications can be observed in present-day tokamaks operation in ELMy H-mode conditions and if they compromise the plasma operation.

Pioneering experimental studies with this respect have been carried out in the TEXTOR device under L-mode conditions in plasmas with He majority [9]. An actively pre-heated limiter equipped with W stripes, pre-exposed in the NAGDIS-I facility to He plasmas providing nanostructured W on one stripe and He nanobubbles in W on another stripe, was exposed to He tokamak plasmas under conditions which shall promote a further growth of W nanostructure and its formation arising from the He nanobubbles, respectively. TEXTOR, operating with a first wall made of graphite and this actively heated, roof-like limiter equipped with the different He pre-damaged W stripes showed no growth of W nanostructures though all three criteria mentioned before for growth were met. Instead in the near scrape-off layer (SOL), W nanostructure erosion by impinging C impurity ions originating from first wall erosion [10] has been observed on the corresponding limiter stripes and deposition by carbon was detected a few centimeters inside the SOL on all W stripes. Thus, in the case of L-mode plasmas the impinging flux distribution of low-Z impurity ions is an additional parameter determining if W nanostructure is growing. The concentration of low-Z impurities, in the case of TEXTOR C with a flux ratio of $\Gamma_C \sim (0.03) \times \Gamma_{(He+D)}$, determines if erosion of W takes place or deposition by low-Z impurities. Comparable studies in a virtual-free low-Z device were executed in [11] in the all-metal tokamak CMOD. Here, indeed the three above mentioned parameters required for W nanostructure formation were fulfilled at a W sample located at the nose of the outer divertor and clear W nanostructure growth was observed within 12 discharges accumulating in 15 s the required He ion fluence. However, the plasma operation was in an ELM-free H-mode, thus without any high energetic ions impinging during an ELM event at the target plate as it will be the case in ITER. Thus, in view of ITER, studies in type-I ELMy H-mode discharges are required to conclude if the balance between W nanostructure growth and erosion [12] is shifted in favour of the nanostructure formation or if net erosion under ELM impact takes place. Studies in PISCES-B simulating ELM-like behaviour by plasma biasing in He demonstrated a clear erosion after single events [13].

Here, we report on experiments carried out in He ELMy H-mode plasmas in ASDEX-Upgrade - a full W-device with occasional use of boronisation and low residual C content [3]. The exposition of W samples in the outer divertor of ASDEX Upgrade aim to investigate in detail (a) the potential growth of W nanostructures on pre-damaged W samples incorporating He nanobubbles and (b) the ELM-induced erosion of thick W nanostructures. The pre-damage of W samples by energetic He atoms was done prior to the tokamak exposure in the neutral beam facility GLADIS providing a set of samples exposed to different He fluence and surface temperature resulting in particular in samples with coral-like W nanostructure and samples with He nanobubbles. The GLADIS operational parameters were selected according to [5] where detailed characterisation of the surface morphology after the adiabatic loading was done by post-mortem analysis. Subsequently, ASDEX Upgrade plasma and surface conditions are selected to induce formation or growth of W nanostructures on these pre-damaged W samples. These experimental conditions in the full metallic environment are close to conditions expected in the divertor of ITER during the He start-up phase [15].

2. Experiment

The experimental approach to study W nanostructure behaviour in He-dominated ASDEX Upgrade plasmas presented here is comparable to the TEXTOR studies [9] employing three steps of W sample treatment: (i) He pre-exposure of W samples in laboratory plasmas (here: GLADIS), (ii) Exposure of pre-damaged W samples in tokamak plasmas (here: ASDEX Upgrade), and (iii) post-mortem analysis of W samples and comparison with the reference morphology (here: IBA and SEM). Fig. 1a shows the set of polycrystalline W samples (T1-T6) after He exposition in GLADIS - corresponding to part (i). Fig. 1b illustrates the arrangement of the same W samples (T1-T6) after He plasma exposition in ASDEX Upgrade - corresponding to part (ii). The purpose of the three experimental parts can be described in the following way:

- Pre-exposure of W samples to a set of different fluences of He particles and surface temperatures in controlled laboratory plasma conditions providing pre-damaged W samples with He nanobubbles at the fluence onset to W nanostructure formation up to fully developed W nanostructures of several micrometer thickness. Here, GLADIS was used for the He pre-exposition [5] in contrast to a linear plasma device in the case of the TEXTOR experiment. The detailed surface morphology differs slightly between GLADIS operating at high He atom impact energies of tens of *keV* inducing a coral-like structure and linear plasma devices operating at low He ion impact energies of tens of *eV* inducing a tendril-like structure [11]. Both however provide a representative nanostructured W surface with comparable properties like high porosity, reduced thermal conductivity etc.
- Exposure of pre-damaged W samples installed in the DIvertor Manipulator (DIM-II) [16] of ASDEX Upgrade located in the outer divertor. The strike-line position is used to expose in sequence different He pre-damaged W samples under different plasma conditions. This utilisation of the strike-line position allows to separate the two main questions: (a) Will W nanostructure formation be initiated on the sample (T2) with already pre-implanted He nanobubbles and initial thin nanostructure formed if the operational conditions are fulfilling the requirements for growth? (b) How will existing thick W nanostructure be modified by tokamak plasma impact? Here, in particular the question of ELM-induced W erosion will be addressed for the

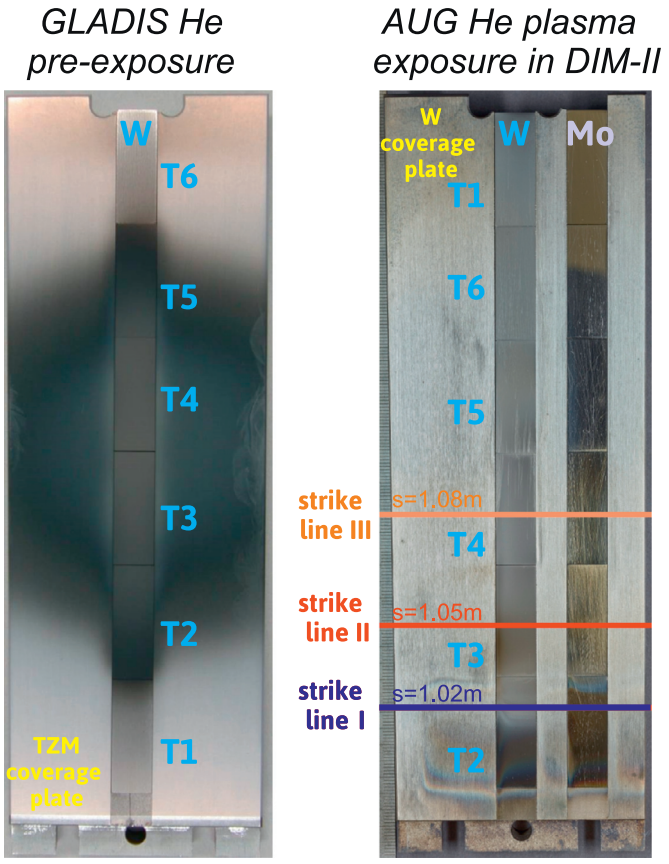

Fig. 1. a) He-exposure arrangement of W samples in GLADIS. b) He-exposure arrangement of W samples in the divertor manipulator of ASDEX Upgrade (AUG) with the three strike-line positions for the different experiments indicated.

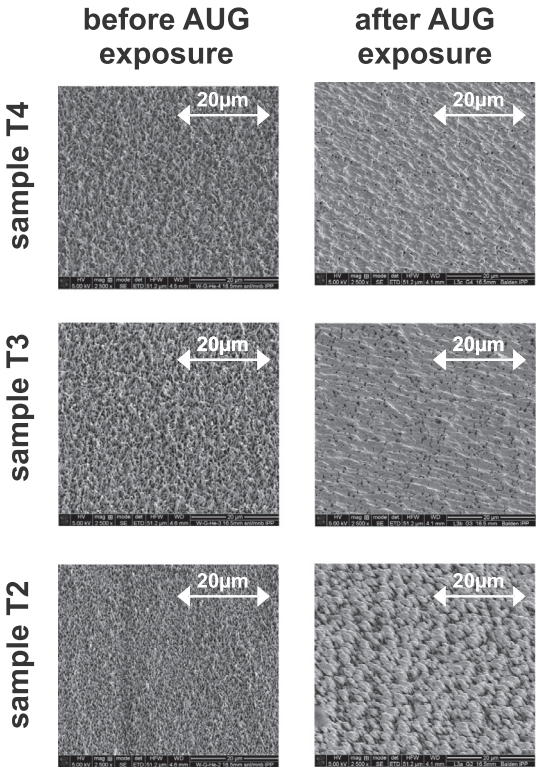

Fig. 2. Left: SEM images of samples T2 (just above the onset of W nanostructure formation), T3 (W nanostructures formed), and T4 (W nanostructures formed) after He bombardment in GLADIS. Right: Comparable SEM images after exposure to He plasmas in ASDEX Upgrade (AUG) visualising changes in surface morphology.

first time in a metallic tokamak environment. The complexity of the latter includes also the material migration from the main chamber into the divertor and within the divertor whereas under normal deuterium plasma conditions the outer divertor leg is representing a net-erosion zone [17]. As reference for the global migration behaviour, a second set of six Molybdenum (Mo) samples of identical dimension is installed at the same poloidal position, but toroidally shifted by 2 cm on the same W coverage plate in DIM-II (Fig. 1b).

- In-situ information about the change of surface morphology during tokamak plasma operation are very limited, i.e. here only a visible camera observation is available (Fig. 3b) recording the integral change of photon emission owing to variation in surface temperature, reflection properties, He recycling and W erosion. Different ex-situ analysis methods like Scanning Electron Microscopy (SEM), Nuclear Reaction Analysis (NRA), Secondary Ion Mass Spectrometry (SIMS) are required to characterise the expected changes in surface morphology, in impurity coverage, W erosion, and He content in W post mortem. Pre-characterisation of W samples is performed by SEM after exposition in GLADIS which allow a direct comparison of W samples before and after tokamak plasma exposure as shown in Fig. 2 for samples T2 and T3 on the left and right-hand-side, respectively. The SEM methodology employing contrast for component analysis is comparable to the analysis reported in [19] on W samples exposed to deuterium plasmas in ASDEX Upgrade.

Table 1
Exposure conditions for the different tungsten samples in GLADIS.

Sample	T3/T4	T2/T5	T1/T6
He flux [10^{21} m^{-2} s^{-1}]	~ 1.7	~ 1.3	0.7
He fluence [10^{24} m^{-2}]	~ 1.0	~ 0.75	~ 0.4
Integral loading time [s]	~ 580	~ 580	~ 580
Peak surface temperature [K]	~ 2300	~ 1800	~ 1300
Impact energy [keV]	37	37	37

2.1. Helium exposure in GLADIS

The He exposition conditions of W samples in GLADIS were comparable to the experimental studies described in [5] where a comprehensive and complete characterisation of the surface modifications of the applied polycrystalline W, also used in this experiment, is done. Six W samples (T1-T6: each of dimension 30 × 12 × 4 mm^3) were embedded in a molybdenum-alloy (TZM) target plate and exposed to the beam at E_{in} = 37 keV of He^0. Fig. 1a shows the geometrical arrangement of the samples as well as implicitly the heat and particle load footprint on the target plate by darkening with maximum incident particle flux and surface temperature in the centre on samples T3 and T4. Though the GLADIS beam profile is not homogeneous and the loading occurs adiabatically, it is possible to describe the averaged exposure conditions for the different samples as summarised in Table 1. W nanostructure of about 2µm thickness are formed on W sample T3 and T4 with a fluence of $\phi \simeq 1 \times 10^{24}$ He^0m^{-2} and at a peak surface temperature of $T_{surf} \simeq$ 2300 K. In particular sample T3 is further used for W nanostructure erosion studies in ASDEX Upgrade. The corresponding values for T2 and T5 are $\phi \simeq 0.75 \times 10^{24}$ He^0m^{-2} and $T_{surf} \simeq$ 1800 K. The strongest gradient in the impinging flux occurs on these two samples: the lower part of T2 and the upper part of T5 are just at the

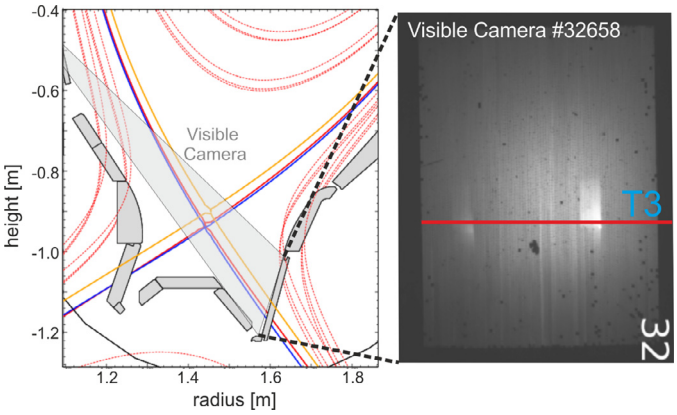

Fig. 3. a) Magnetic configuration in the divertor for the three phases of exposure and the line-of-sight of the camera on the divertor manipulator location. b) Image of divertor manipulator plates during plasma exposure in the visible spectral range.

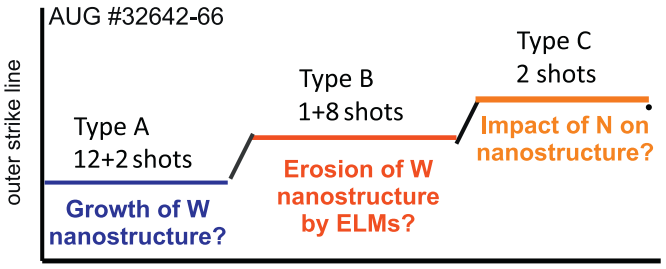

Fig. 4. Schematic arrangement of the three exposure conditions, number of discharges, and outer strike-line positions.

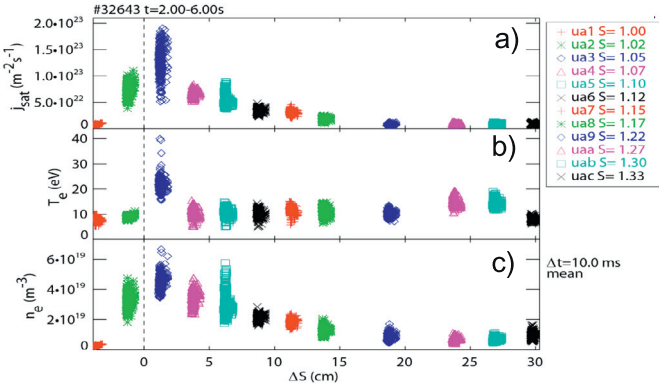

Fig. 5. Plasma conditions in the near scrape-off layer region measured by an array of Langmuir probes for discharges in exposure conditions A: a) ion saturation current, b) electron temperature, and c) electron density as function of the change of the s-coordinate with respect to the magnetic outer strike-line position.

threshold for W nanostructure formation, but with significant He nanobubbles incorporated in the W matrix whereas the upper part of T2 and the lower part of T5 already fully develop the typical coral nanostructure of W. The centre of sample T2 has been targeted in the ASDEX Upgrade experiment by the outer-strike line to study the formation and growth of W nanostructures as described below. However, due to the present flux and temperature profiles owing to the footprint in the He pre-exposition, a wider range of W nanostructures with different height, density, and thickness will result. Representative SEM images of the microstructure surface of sample T2, T3, and T4 after GLADIS exposure are shown in Fig. 2a.

2.2. Exposure in ASDEX Upgrade He plasmas

H-mode experiments in ASDEX Upgrade have been carried out in lower single null configuration (Fig. 3a) at a toroidal magnetic field of $B_t = 2.5$ T, a plasma current of $I_p = 0.8$ MA, and auxiliary power of about $P_{aux} = 8.5$ MW consisting of a mixture of neutral-beam injection in He and H of minimum 2.1 MW, ion cyclotron resonance heating (ICRH) of up to 3.9 MW, and central electron-cyclotron resonance heating of about 2.6 MW. The operating gas and main plasma species was He with a purity of typically $\frac{n(He)}{n(He)+n(D)+n(H)} > 0.8$. These He plasmas were executed directly after a fuel species exchange experiment from D into He by ion-cyclotron wall conditioning (ICWC) plasmas. It should be noted that the last boronisation on B_2D_6 in ASDEX Upgrade was just 2 experimental days with about 175 plasma seconds before the ICWC change over in 24 discharges took place, thus the first He plasmas might still be affected by the boron coverage of the first wall and its conditioning effect [20]. The typical core plasma conditions of these He plasmas during the H-mode flat-top phase of about 7 s duration are: electron density $n_e^c \simeq 9.5 \times 10^{19}$ m^{-3} and electron temperature $T_e^c \simeq 3.0$ keV.

The goal of the exposure to predominately He plasmas is to investigate (a) the potential growth of W nanostructures on pre-damaged W samples incorporating He nanobubbles (type A plasmas / sample T2), (b) the erosion of thick W nanostructures (type B plasmas / sample T3), and (c) the impact of Nitrogen (N) on the W nanostructure (type C plasmas / sample T4). Thus, three studies in ASDEX Upgrade were executed in one experimental day consisting of 25 diverted plasmas (#32642 – 32466) by variation of the outer strike-line located on three different He pre-exposed W samples installed in the divertor manipulator at the low field side as shown in Fig. 1b. The correlation between plasma type, outer strike-line position, and W sample is depicted in Fig. 4. The core plasma conditions are similar apart from the strike-line position varied between $s = 1.02$ m (type A), $s = 1.05$ m (type B), and $s = 1.08$ m (type C) as well as the lower He gas injection rate during type B plasmas though controlled fuelling was compromised by He outgassing from the W first wall. The two plasma discharges of type C had additional N_2 blibs. We assume that the different strike-point positions and the order of experiments allow a separation of the three experimental parts. No significant impact on the plasma-exposed W sample surfaces is expected when the outer strike-line is moving upwards, from type A to type C plasma, into the direction of SOL which leaves the modified W surface in the private-flux region (PFR) under negligible power and ionic particle load.

- Type A - the W nanostructure growth regime. In this case the strike-line is positioned at the poloidal divertor coordinate $s = 1.02$ m and the corresponding time averaged radial profiles for the local electron temperature T_e, electron density n_e, and the ion saturation current density j_{sat} are shown in Fig. 5. Assuming that singly ionised He ions are impinging the outer divertor target plate, the peak impact ion energy can be estimated to be about $E_{in} = 150$ eV, assuming $k_B T_e = k_B T_i$, and thus clearly above the required 20 eV. The peak ion flux density at the location of the strike line amounts $j_{sat} = 2.0 \times 10^{23}$ m^{-2}s^{-1}, 80% of which can be attributed to He ions. In 14 discharges executed in scenario A an integral plasma exposure time of about 100 s has been reached. This leads to an achieved He ion fluence of $\phi = 1.6 \times 10^{25}$ m^{-2} and thus one order above the threshold required for W nanostructure growth from undamaged W samples. There has been no direct measurement of the surface temperature at the location of the DIM-II, however, infrared measurements at different toroidal location at normal W divertor target plates suggest at least a temperature of 800 K of standard W PFCs with good thermal conductivity. The W samples installed in the DIM-II have a poor thermal contact to the baseplate. The surface temperature is therefore assumed to be sig-

nificantly above 1000 K. Visible camera images (Fig. 3b) indeed observe strong thermal radiation at the poloidal location of the exposed W sample whereas the W covering plate shows no such radiation though receiving the same power and particle load at the same poloidal location, but just slightly toroidally shifted. It should be noted that the H-mode performance was overall poor in the case of Type A plasmas (pedestal conditions: $T_e^{ped} \simeq 330$ eV and $n_e^{ped} \simeq 6.15 \times 10^{19}$ m^{-3}) with an ELM frequency in the kHz range suggesting type III like ELMy H-mode with moderate intra-ELM He ion impact energies and low ELM-induced W sputtering as observed before in D plasmas using standard W PFCs [3].

Overall, the experimental conditions in the first part of the experiment (type A) are fulfilling all the requirements for W nanostructure formation and growth in ASDEX Upgrade. However, visible inspection of the W sample T2 directly after end of the plasma exposure suggested a change in reflection properties from a blackened to a shiny W surface indicating modifications in the surface morphology, but no clear signature of W nanostructure formation.

- Type B - the W nanostructure erosion regime. In this second set of 9 comparable discharges, the aim is to study the ELM-induced W nanostructure erosion. The outer strike-line in this second set of discharges is positioned at $s = 1.05$ m on W sample T3 employing an about 2 µm thick W nanostructure as top surface. The averaged edge plasmas conditions T_e, n_e, and j_{sat} reflecting mainly the inter-ELM phase are comparable to type A plasmas as well as T_{surf}. The corresponding fluence ϕ in the about 63 plasma seconds amounts to 1.0×10^{25} He^{+}m^{-2} and would still potentially allow W nanostructure growth between ELMs. The fuelling rate in this second set of plasmas is reduced to half of the value of type A plasmas in order to provide a more pronounced H-mode with lower ELM frequency (120 Hz) and larger energy drop per ELM. The impact energy of presumably He^{2+} from the pedestal region arriving at the outer target plate in less than 1 ms is substantially above the sputtering threshold of W. Assuming a relationship between pedestal energy and impact energy according to the free-streaming approach as recently observed in JET-ILW in [22], the impact energy in these He plasmas is assumed to be above 1 keV. This would indeed allow the expected competition between W nanostructure sputtering by ELM impact under conditions otherwise favouring W nanostructure growth. The visual inspection of sample T3 reveals also a shiny W surface, suggesting a change of the surface morphology with reduced surface roughness - the origin of which will be discussed in the next section.
- Type C - the impact of N on W nanostructure. N_2 was injected into two He plasmas with the outer strike line at $s = 1.08$ m impacting on sample T4 with thick W nanostructure. The interaction of N with the W morphology will be studied in future by post-mortem analysis.

3. Discussion

The first observation after exposure of the six He pre-damaged W samples to ASDEX Upgrade may be summarised in the following way: change of surface morphology and roughness on all W samples starting at PFR, passing the three applied strike-line positions, and ending in the SOL (Fig. 1b). Different post-mortem analysis techniques, i.e. ion beam analysis (IBA) and scanning electron microscopy (SEM) combined with focused ion beam (FIB) cutting, are applied to obtain physics information for interpretation. SEM images of subareas (50 µm × 40 µm) on samples T2, T3, and T4 before (left-hand side) and after ASDEX Upgrade exposure (right-hand side) are depicted in Fig. 2 showing the mentioned surface modification with reduction of surface roughening and in general

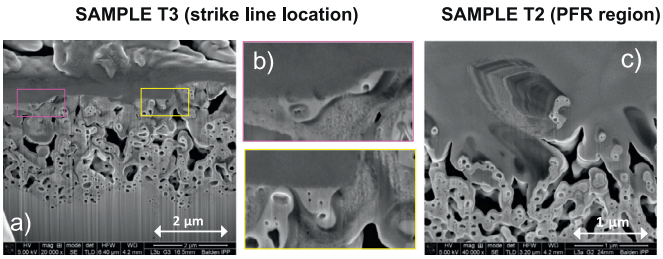

Fig. 6. a) Cross-section of a tungsten nanostructure sample after ASDEX Upgrade plasma exposure. b) Enlarged images to show detailed structure with sharp cuts from erosion as well as homogenous deposition of predominantly W. c) Focused ion beam cut of a tungsten sample showing the deposition of a manifold of individual layers corresponding to the number of discharges.

absence of the coral-like W nanostructure. Cross-sectioning with FIB and SEM reveals that the observed surface modification is due to an almost homogeneous coverage by a $0.5 - 1.0$ µm thick deposition layer as shown e.g. in Fig. 6a for sample T3. Fig. 6c shows a cut through the deposition layer of the upper part of sample T2 indicating more than 20 individual substructures suggesting that effectively each of the 25 executed discharges is contributing to the deposition. Indeed both high-Z (W) and low-Z species are present in this deposition layer according to contrast analysis with SEM. The chemical composition and distribution of the deposition layer has been determined by IBA and identified to be a mixture of B, C, D as well as W; energy dispersive X-ray spectroscopy (EDX) confirms the significant appearance B and C. Fig. 7a shows the poloidal deposition profiles of B, C, D on the different He pre-damaged W samples and Fig. 7b the corresponding profiles on the polished Mo reference samples. In addition Fig. 7b includes also W deposition profile on the Mo samples. Fig. 7a shows the He ion flux distribution, thus the distribution of impinging fuel species measured by Langmuir Probes for type B plasmas with the outer strike line located at 1.05 m. Common for the deposition pattern of all species on the pre-damaged W and the Mo reference samples is the strong deposition deep inside the PFR region. Indeed, there is only very limited deposition of B on the polished Mo samples above $s = 1.02$ m which is the lowest position of the outer strike line in the executed discharges. Thus, one can conclude that significant deposition is absent in the SOL in the case of polished surfaces with low surface roughness. In contrast, in the case of samples with W nanostructure, which have fully established coral-structure between approximately $x = 20$ mm and $x = 110$ mm in poloidal direction, a strong deposition of B and C can be measured without any significant D embedded in the deposit. In the SOL, the B deposition profile follows the impinging He ion flux profile whereas the C deposition profile is flat in the range of the established W nanostructure including three minor peaks at the intersection of samples T2/T3, T3/T4, and T4/T5. Re-erosion from this area of complex surface morphology by physical sputtering is reduced, whereas chemical erosion still can occur which might be the cause for the difference between B and C. Overall the averaged B to C ratio in the deposit is approximately two. Unfortunately, it is not possible to provide from this measurement the ratio of low-Z impurities to the also present impinging W ion flux which has been measured on the Mo reference sample.

W samples with pre-formed W nanostructures with large surface roughness, large effective surface area, and high porosity act as a kind of catcher for the impinging ions from the plasma. Quickly, after establishment of a thin deposition layer (B, C, W), the existing W nanostructure is covered and protected from further erosion. Every additional discharge is inducing another layer and contributing to the observed deposition with more than 20 identified layers. Contrary, in the case of the polished Mo reference sur-

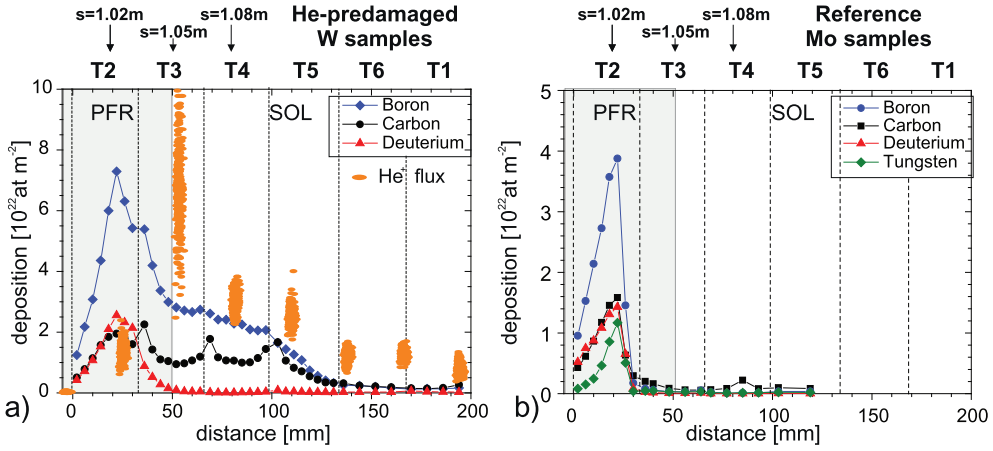

Fig. 7. a) Poloidal distribution of B, C, and D along the six tungsten samples installed in the divertor. The He ion flux distribution is shown accordingly as reference for the impinging flux. b) Deposition of W as well as B, C, and D on the reference poloidal sample stripe made of Mo.

face are the impinging low-Z particles either re-eroded or reflected from the high-Z surface - similar to observations made in TEXTOR with C on W [21] - and no effective deposition layer growth can occur. One can assume that geometrically on both poloidal sample stripes, the W and Mo one, the same impurity flux distribution is impinging, thus, the difference in the two deposition profiles on the stripes provides effectively the fluence of impinging impurity ions accumulated over all discharges. The near SOL region of the outer divertor leg is under normal D plasmas conditions in ASDEX Upgrade a clear net-erosion source of W [17], but in the present He plasmas the balance between erosion and deposition has changed towards deposition. Indeed on the polished Mo samples it is almost fully balanced and in the case of the W nanostructure with larger surface roughness re-erosion is further reduced. The outer divertor is locally, at the location of the W stripes, transferred into a net-deposition zone for C and B. The high level of B in the deposit is caused by the boronisation which took place about 175 plasma seconds before the actual experiments. The protective B layer in the main chamber is continuously eroded by plasma bombardment and the released B is ionised and transported into the divertor as previously observed in D [18]. The B erosion in the main chamber is larger in the present He plasmas than in D plasmas under similar plasma conditions due to higher mass and effective charge of the impinging ion. The level of C is in the normal range of ASDEX Upgrade plasmas.

The observed W in the divertor is also a result of main chamber - limiters and heat shield - erosion, but due to ELM impact as reported for D plasmas before [14]. The W source in the present He plasmas is significantly higher than in D due to a) the higher mass of the impinging projectile and b) the higher ionisation stage of impinging He in comparison with D, and finally due to the use of ICRH antenna [14]. The transport of higher ionisation stages of W from the main chamber into the divertor then results in the deposition on both the W nanostructure samples as well as the Mo reference samples.

Focusing again on the initial experimental goals of the He plasmas of type A and type B, one can summarise the observations and conclude:

- Type A - the W nanostructure growth regime. No signature of W nanostructure formation or growth under the given experimental conditions in ASDEX Upgrade though the proper conditions for W nanostructure formation with respect to ion impact energy, fluence and surface conditions are met in these plasmas of type A and the outer strike line positioned on sample T2. SEM of cross-section cuts of the sample reveal a deposition layer consisting of B, C, and W with high density on the strike-line area on sample T2. Strongest deposition is observed below the actual strike-line position in the PFR and also on the reference Mo samples as visible in Fig. 1b). Potential reason might be related to $\vec{E} \times \vec{B}$ drifts in the divertor as suggested for D plasmas in similar configuration by [24]. The overall D content is negligibly low in the SOL, but substantial - up to 15% of the codeposit - in the deposition enriched region in the PFR.
- Type B - the W nanostructure erosion regime. Only moderate erosion of samples with W nanostructure was observed close to the outer strike-line region on sample T3 as depicted in Fig. 6a. Fig. 6b shows a SEM image of a corresponding cross-section cut of W sample T3 with initially about 2 µm thick W nanostructure. The top part of the coral-like structure is flattened and overlaid by a homogeneous deposition layer. There is no indication of melting of the top part of the nanostructure, but rather local erosion of individual “W-corals” took place which effectively smoothed the microstructure while the deposition covered the whole surface area. The erosion is determined by ELMs carrying He^{2+} with about $1keV$ impact energy from the pedestal to the outer target plate similar to observations in JET-ILW [22]. Even if the sputtering yield for nanostructured W is slightly lower than for standard W as reported by PISCES-B for low impact energies [12], the erosion yield dependence as a function of the impact energy can be assumed to be comparable at energies above *keV* to standard W. Although every ELM impact indeed fulfils conditions for W erosion by physical sputtering, the erosion process was in the present case in general overcompensated by local deposition - predominantly occurring between the ELMs. It should be noted that the original coral-like structure on T3 remains detectable by SEM in a very low fraction of surface area close to the strike-line position. Thus, in this case, the flux of ELM-induced sputtered particles is in balance with the flux of depositing particles.

The interplay between local erosion of W nanostructures at the strike-zone and deposition in the SOL observed here is in accordance with previous TEXTOR W limiter experiments in He-dominated plasmas [9] though latter were executed in ELM-free conditions and solely influenced by C impurities. Both experiments stress the universal character and the importance of the low-Z impurity flux in the local balance equation between erosion and deposition on W nanostructure surfaces.

4. Conclusion

In He ELMy H-mode plasmas in ASDEX Upgrade no growth of W nanostructures takes place despite the fact that the operational conditions fulfil the requirements for their formation and growth. Thus, the formation of W nanostructures depends in addition to the known dependencies on the fluence of He ions, their impact energy, and the surface temperature [6,15] also on the impinging flux of impurities such as boron and carbon as well as W ions onto the outer W target plate. Neither W nor intrinsic impurity ions have in the case of ASDEX Upgrade their origin in the divertor, but are a result of main chamber erosion - W PFCs and B from boronisation - and adjacent material transport towards the divertor. In the case of ELMy H-mode plasmas in ASDEX Upgrade, the plasma outflux of B, C, and W ions compensates the W erosion flux and shifts the local balance in the outer divertor from net-erosion into net-deposition though ELM-induced W sputtering close to the strike-line takes place. Moreover, the highest deposition of low-Z and high-Z species is located in the private-flux region indicating either a local transport mechanism from the scrape-off layer into the private-flux region or significant re-erosion at the strike-line location. This general erosion and deposition pattern is not solely related to the W surface modifications as a similar pattern can be observed on reference polished Mo samples at the same poloidal position, but to the global transport of impurities from the main chamber into the divertor as seen before in [23]. In the case of the samples with W nanostructure, surface roughness and porosity increases strongly the degree of deposition with respect to the polished Mo surfaces and visualises effectively the impinging ion fluence.

It is evident that the main chamber W source in these ICRH-heated He plasmas is significantly higher than in H-mode D plasmas in order to cause the shift in the local W erosion and deposition pattern. Fast impurity ions and deuterons (i.e. intra-ELM) were identified before [14] as the main cause for W erosion at limiters and heat shields in the main chamber. The increase of the projectile mass of the main fuel species from D ($m = 2$) to He ($m = 4$), the lower sputtering threshold, and the higher charge state of He ions hitting the wall are contributing to the increased W wall source in He. However, further post-mortem analysis needs to be done to get a further insight in the interplay between the different parameters for W growth and the observed net-deposition of W by W, B and C along the full outer target plate including the Mo reference samples. Moreover, local spectroscopy at the location of the divertor manipulator would be advisable in order to measure in-situ the different flux contributions.

The observed deposition contribution of B and C in ASDEX Upgrade can be seen as proxy to intrinsic beryllium (Be) in He plasmas in ITER. The initial formation of W nanostructures at critical areas in the W divertor fulfilling the standard criteria for W growth can be hindered if the local erosion/deposition flux balance is in favour of deposition due to stronger Be main chamber sources in He in contrast to D. Indeed the Be erosion source under He impact is expected to be at least twice as large as in D. Repetition of the experiment at JET-ILW in He plasmas would be advisable to investigate a change in the primary Be source and migration pattern [25] as well as to provide input for modelling codes, WallDYN [26] for the global migration pattern and the balance in the divertor, and ERO [27] for the local ELM-induced W sputtering effects. Subsequently, more detailed studies on W nanostructure erosion due to ELM impact need to be executed at ITER-relevant ELM impact energies and ion fluxes before further modelling of the W surface morphology changes can be done.

References

[1] R. A. Pitts, et al., 2013. 55th Annual Meeting of APS Division of Plasma Physics, Denver, USA, WE1.00001.
[2] V. Philipps, J. Nucl. Mater. 415 (2011) S2.
[3] R. Neu, et al., IEEE Trans. Plasma Sci. 42 (2014) 552.
[4] M.J. Baldwin, R.P. Doerner, Nucl. Fusion 48 (2008) 035001.
[5] H. Greuner, et al., J. Nucl. Mater. 417 (2011) 495.
[6] S. Kajita, et al., Nucl. Fusion 49 (2009) 095005.
[7] M. Baldwin, et al., Nucl. Fusion 51 (2011) 103021.
[8] T.J. Petty, et al., Nucl. Fusion 55 (2015) 093033.
[9] Y. Ueda, et al., J. Nucl. Mater. 415 (2011) S92.
[10] S. Brezinsek, et al., Phys. Scr. T167 (2011) 14067.
[11] G.M. Wright, et al., Nucl. Fusion 52 (2012) 042003.
[12] D. Nishijima, et al., J. Nucl. Mater. 415 (2011) 230.
[13] D. Nishijima, et al., J. Nucl. Mater. 434 (2013) 230.
[14] R. Dux, et al., J. Nucl. Mater. 390–391 (2009) 858.
[15] Y. Ueda, et al., J. Nucl. Mater. 442 (2013) S267.
[16] A. Hermann, et al., Fus. Eng. Design 98 (2015) 1496.
[17] M. Mayer, et al., Phys. Scr. T138 (2009) 014039.
[18] A. Hakola, et al., J. Nucl. Mater. 415 (2010) S226.
[19] M. Balden, et al., J. Nucl. Mater. 438 (2013) S220.
[20] V. Rohde, et al., J. Nucl. Mater. 363365 (2007) 1369.
[21] A. Kreter, et al., Plasma Phys. and Control. Fusion 48 (2006) 1401.
[22] C. Guillemaut, et al., Plasma Phys. Control. Fusion 57 (2015) 085006.
[23] A. Hakola, et al., Phys. Scr. T167 (2016) 014026.
[24] A. Hakola, et al., - these proceedings.
[25] S. Brezinsek, et al., Nucl. Fus. 55 (2015) 063021.
[26] K. Schmid, et al., J. Nucl. Mater. 463 (2015) 66.
[27] A. Kirschner, et al., J. Nucl. Mater. 463 (2015) 116.